Mobile Netw Appl (2007) 12:438–449
DOI 10.1007/s11036-008-0043-7

A Markov Model for Indoor Ultra-wideband Channel with People Shadowing

Ruonan Zhang · Lin Cai

Published online: 22 April 2008

Abstract For an indoor ultra-wideband (UWB) communication system, the line-of-sight (LOS) between the transmitter and receiver may be frequently blocked by moving people. Blocking of LOS may significantly affect the quality of service of on-going UWB communications. Based on the Angular Power Spectrum Density and the human blocking models, we build a packet-level UWB channel model considering the shadowing processes based on a Finite-state Markov Chain. The model is simple enough to be incorporated into existing network simulators like NS-2 and it can be used to facilitate protocol design and quality of service analysis for UWB based wireless personal area networks.

Keywords channel model · UWB · angular power spectrum density

1 Introduction

To provide the 'last-meter' connectivity inside homes, broadband home networks have raised wide attention in both academia and industry. Wireless Personal Area Networks (WPANs) using Ultra-wideband (UWB) technologies have shown great potential as future home networks, because a) UWB achieves very high data rate (> 100 Mbps) at very low transmission power (≤ −41.25 dBm/MHz) and interference to other wireless systems; b) UWB's relatively short transmission range and high attenuation by barriers such as concrete walls are desirable characteristics to service providers, who do not want their broadband signals to be shared by other (non-subscribing) homes; and c) using wireless technologies can avoid house rewiring, which is critically important to both service providers and consumers.

The indoor UWB channel is crucial to determine the achievable performance and Quality of Service (QoS) of the UWB home networks [5]. Particularly, the achievable throughput depends on the packet error rate (PER), which in turn depends on the received signal-to-noise ratio (SNR). Because of the closed space and dense scatters in home, an indoor broadband wireless channel has typically severe multipath effect and time-varying attenuation (fading). With extensive efforts in measuring the physical indoor channels, (e.g., in [1, 2] and [3]), the IEEE 802.15.3a WPAN group has standardized the UWB channel models, known as the 3a [4] and 4a model [6]. The 3a model has been widely used for testing indoor UWB system proposals and system simulations in the literature.

However, using the 3a channel model, the waveform simulation of transmitting every bit over the wireless channel comes at a high computation cost and a very long execution time. Therefore, a packet-level channel model of the UWB transmission system is more desirable for simulation and design of the upper layer protocols. By capturing the network activities on a packet-to-packet basis, the packet-level channel model directly generates the packet error profile for a wireless link. It can be used to analyze the network protocol and

R. Zhang · L. Cai (✉)
Department of Electrical and Computer Engineering,
University of Victoria, Victoria, British Columbia
V8W 3P6, Canada
e-mail: cai@ece.uvic.ca

R. Zhang
e-mail: rzhang@ece.uvic.ca

QoS performance, like link throughput, delay, etc., in a practical transmission environment. Therefore, a packet-level channel model of UWB systems is of great interest and it can facilitate the analysis and simulation of WPANs.

A packet-level channel model provides the PER on a packet basis according to the statistical properties and time-variation of the practical wireless channel. The 3a or 4a report does not explicitly define the time-variance property of the UWB indoor channel, although it has been reported by Molisch [7] and Schell [8]. To the best of our knowledge, there is no packet-level model for UWB indoor channels which considers their time-variance property in the literature.

Since the indoor propagation environment is very complicated, it is very difficult if not impossible for a single model to describe all possible variation of the UWB channel. We category the indoor propagation environments into the following four different scenarios. Each scenario should be treated separately and they lead to different mathematical models. With the first scenario, the transmitter (Tx), receiver (Rx) and scatters all remain stationary, or the moving scatters are far away from the line-of-sight (LOS) between the Tx and Rx. In this case, the channel is stationary, or the movement of scatters does not significantly affect the transmitted signal. Therefore, the channel is a time-invariant frequency-selective channel with AWGN, and the error probability remains constant. With the second scenario, the Tx, Rx or scatters are moving and the LOS or NLOS condition remains unchanged. The channel can be regarded as a WSS-US channel and undergoes small-scale fading. The fading of the channel can be described stochastically, for example, using the Rayleigh or Log-normal distribution to model the fading of each tap in the channel impulse response (IR). The correlation of the fading can be estimated based on the movement speed. With the third scenario, the Tx and Rx are stationary, but an obstacle (most likely a person in an indoor environment) moves and intercepts the LOS. Because the LOS, the most significant path, is shadowed off, such variation can be regarded as large-scale fading. The last scenario is that the Tx,Rx and obstacles are moving, and the LOS or NLOS condition changes due to mobility or shadowing.

The third scenario is very common for indoor environments, where people may frequently penetrate the LOS of an ongoing wireless link. In addition, the shadowing effect is significant for UWB transmissions, because for UWB communications with several hundred megabits per second data rate, even a half second shadowing due to moving obstacles can affect more than hundred megabits data. In addition, WPANs typically carry the high data rate multimedia streaming traffic which is delay and loss sensitive. Even a short time shadowing degrades the quality of the ongoing flows severely. Therefore, this paper addresses the third scenario, and our results can be extended to study the fourth scenario in the future.

The main contributions of this paper are two-fold. First, we analyze the shadowing processes of UWB channels based on angular power spectrum density (APSD). Second, a continuous-time Markov model to describe the channel shadowing processes at packet-level is proposed. This model can be used for the simulation and performance/QoS analysis of UWB networks, incorporating the effects of moving people in a realistic indoor environment.

The remainder of the paper is organized as follows. In Section 2, the APSD is presented for the channel IR of UWB 3a channels. In Section 3, the shadowing effect of a people's body on the LOS of UWB channel is analyzed based on the APSD and shadowing model. The continuous-time Markov model for the time-varying UWB channel due to people shadowing is proposed in Section 4. Section 5 gives an overview of the MB-OFDM UWB schemes and presents in detail the formulation of the link performance. The numerical results of the shadowing effect, the parameters of the Markov model and the link performance with shadowing are given in Section 6. Section 7 concludes the paper and future work.

2 The APSD of UWB channel IR

The effect of shadowing on LOS can be estimated based on the APSD, because the shadowing effect occurs when some of the incident angles of the signal are obstructed by the obstacle and only the energy from other un-blocked angles can be captured by the receiver. Therefore we first analyze the distribution of the received power over the angle-of-arrival. Molisch in [7] suggested a simplified model of the angular distribution of the energy of each tap in the channel IR. Here, we extend Molisch's method to investigate the effect of LOS shadowing. This section analyzes the azimuth of incident energy based on the UWB channel specified by the standard 3a channel model [4].

2.1 UWB 3a channel model

With closed space and dense scatters, the indoor UWB channel contains many resolvable multipath components. The channel model specified in the IEEE

802.15.3a [4] standard is based on S-V model [1] with small modifications, which is composed of a serials of delayed, attenuated (or faded) taps or rays. The multipath arrivals are grouped into cluster arrivals and ray arrivals within each cluster, as expressed by:

$$h_i(t) = X_i \sum_{l=0}^{L} \sum_{k=0}^{K} \alpha_{k,l}^{i} \delta\left(t - T_l^i - \tau_{k,l}^i\right) \tag{1}$$

where $\alpha_{k,l}^i$ denotes the gain of the k-th multipath component in the l-th cluster, T_l^i is the delay of the l-th cluster, $\tau_{k,l}^i$ is the delay of the k-th path in the l-th cluster relative to the cluster arrival time, X_i represents the log-normal attenuation, and i refers to the i-th realization. The cluster arrivals and the path arrivals within each cluster are modeled as Poisson processes with rate Λ and $\lambda(\lambda > \Lambda)$, respectively. The cluster and ray arrival rates depend on particular environments. The multipath gain coefficients are modeled as independent random variables and log-normally distributed as follows:

$$20\log 10\left(|\alpha_{k,l}^i|\right) \sim N\left(\mu_{k,l}, \sigma_1^2 + \sigma_2^2\right). \tag{2}$$

This is because the large bandwidth of UWB signals significantly increases the ability of the Rx to resolve the different reflections in the channel. As a result, the central limit theorem argument used to justify a Rayleigh distribution for the received signal envelope in the original S-V model may not be valid.

The behavior of the averaged power delay profile (PDP) is

$$\Omega_{k,l} = E\left[|\alpha_{k,l}^i|^2\right] = \Omega_0 e^{-T_l/\Gamma} e^{-\tau_{k,l}/\gamma}, \tag{3}$$

where Ω_0 is the mean energy of the first path of the first cluster. Equation 3 reflects the exponential decay of each cluster (with decay factor of γ), as well as the decay of the total cluster power (with factor Γ), with delay. The power of the multipath components are normalized such that $\Sigma_{l=0}^{L}\Sigma_{k=0}^{K}|\alpha_{k,l}^i|^2 = 1$.

Finally, the total attenuation, X_i, is also modeled as log-normal random variable by:

$$20\log 10(\mathrm{X_i}) \sim N\left(0, \sigma_x^2\right) \tag{4}$$

The above parameters in the model ($\Lambda, \lambda, \Gamma, \gamma, \sigma_1$, σ_2 and σ_x) are defined by trying to match the important statistical characteristics of the channel model output to the characteristics of actual measurements. The model of CM1 is used throughout this work because it is the scenario with LOS existing between the Tx and Rx.

2.2 The analysis of APSD

The angular power distribution, pdf(θ), refers to the probability density of power arriving at angle θ. It describes the distribution of power over the incident angles. Due to the multipath components arriving at the receiver with increasing delay, the channel IR is composed of a number of delayed taps, as described by the 3a model in Eq. 1. The power of each tap is composed of rays coming from different angles with the same delay and thus each tap has its own angular power distribution. Therefore, the distribution is a function of delay, expressed as [7]:

$$\mathrm{pdf}(\theta,\ \tau) = \begin{cases} \mathrm{rect}\left(\dfrac{2\pi\tau}{\tau_{\max}}\right) & 0 < \tau < \tau_{\max} \\ \dfrac{1}{2\pi} & \tau > \tau_{\max} \end{cases} \tag{5}$$

where θ is the incident angle with respect to the LOS component and τ is the delay of the tap. rect$(\cdot)$ is the rectangular function. The pdf$(\theta,\ \tau)$ is the energy angular density of the signal received at the moment of delay τ, and it also is the probability density function by which the received power at delay τ distributes over a certain angular spread, which is $\phi = \min\{2\pi\tau/\tau_{\max}, 2\pi\}$. Figure 1 shows the angular power distribution pdf$(\theta,\ \tau)$.

The energy distribution model shows that the power angular spread increases with delay. For the taps with delay $\tau < \tau_{\max}$, the energy distributes uniformly over the angular range of $\left[\frac{-\pi\tau}{\tau_{\max}}, \frac{\pi\tau}{\tau_{\max}}\right]$, while for the taps with delay $\tau > \tau_{\max}$, the energy distributes uniformly over $[-\pi,\ \pi)$. This angular distribution is reasonable and consistent with the 3a channel model. The taps with short delay should travel through short paths and arrive at the receiver within an angular range close to the LOS direction. At the same time, because of the less path loss and reflection, they should have more energy, which is consistent with the exponential decaying

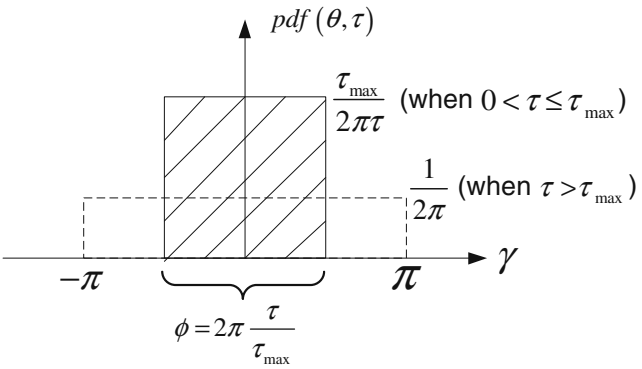

Figure 1 The angular power distribution

model in 3a. Particularly, the LOS component has the smallest delay and it does not distribute over any angles. On the other hand, the taps which have long delay, normally undergo long paths and more reflections. Thus, the incident range of them should be large, like $[-\pi, \pi)$ and they have less energy due to reflection and path loss.

The composite power distribution, or the APSD, refers to the total power received at a certain incident angle, and can be expressed as:

$$P(\theta) = \int_0^\infty \text{pdf}(\theta, \tau)\text{PDP}(\tau)d\tau \tag{6}$$

where $\text{PDP}(\tau)$ is the PDP of the IR of the UWB channel, which is the $|\alpha_{k,l}|^2$ and generated by the 3a model. $P(\theta)$ gives the total energy that the receiver captures at angle θ, since the integral sums up the energy received on the angle θ at all the delay moment τ. The parameter $\tau_{\max}$ should be chosen such that the RMS angular spread of $P(\theta)$ is 32 degree, the average value of the practical measurements in [2] and [3].

The basic steps to obtain the APSD are summarized as follows:

1. Create a random channel realization, with a certain power ascribed to each tap. The CM1 of 3a channel model is used because it describes the scenario of LOS existing.
2. For each delay tap, compute the angular power density $\text{pdf}(\theta, \tau)\text{PDP}(\tau)$ as in Eq. 6 (rectangle pdf with width increasing with delay).
3. Identify the taps whose angle spread cover the incident angle θ, because these taps have the contribution to the total power at this azimuth.
4. Add up all the angular power density of the taps identified in the last step and obtain the total power density at θ.

As described in Subsection 2.1, the channel IR is a stochastic process. The APSD of the UWB channel is calculated and averaged using the 100 channel IR realizations provided by the IEEE 802.15 group, which are generated by the 3a CM1 model and dumped into a trace file. The averaged APSD is shown in Fig. 2. Each of the channel IR is normalized to have a unit total power.

3 LOS shadowing model for UWB channel

We will use the setting of people's shadowing procedure as suggested in [7] and [8], which was also recommended by the IEEE 802.15.3a group to study the time variance of UWB channels. As described in Section 1, the scenario is the shadowing process of the UWB channel with stationary transmitter/receiver and a single obstacle, normally a person, moving through the LOS and thus blocking off the most significant power contribution. The channel model for the shadowing process and the analytical results are given below, which have not been reported in the literature yet.

As shown in Fig. 3, a person moves along a path at random speed v, e.g., with the average speed of $\bar{v} = 0.5$ m/s (the pedestrian speed) and penetrates the LOS. For simplicity of presentation, we consider the path is perpendicular to the line connecting the Tx and Rx, with a distance of D from the receiver at the crossover. (If the movement direction is not perpendicular to the line connecting the Tx and Rx, v equals

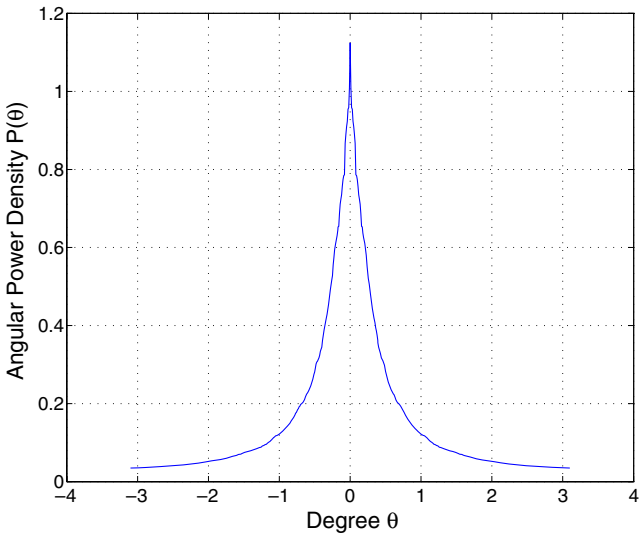

Figure 2 The APSD

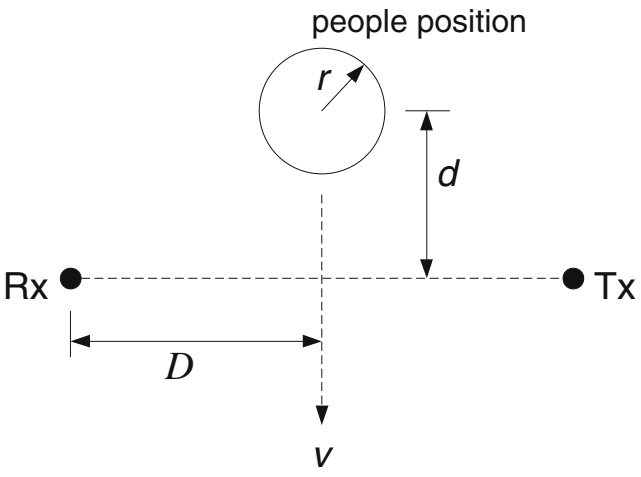

Figure 3 Model of LOS blocking

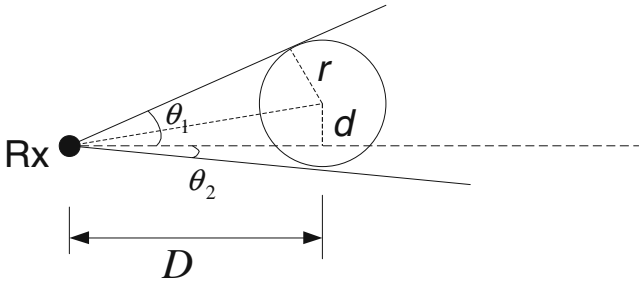

Figure 4 Computation of LOS blocking angular range

$v' \sin\beta$, where v' is the speed of the scatter, and β is the angle between the direction of the velocity and the LOS line.) The person is modeled as a cylinder with radius of $r = 30$ cm, as an approximation of a human body. This model was actually used by [8] in the channel measurement setting. They just used a tank of water to emulate a human body, as a large percentage of the human body is composed of water.

As the person steps toward the LOS, he shadows off certain angular ranges, from which the transmission power cannot reach the receiver. The angular ranges of shadowing can be obtained from simple geometrical computations. For example, the angles θ_1 and θ_2 in Fig. 4 equal $\arctan\left(\frac{d}{D}\right) + \arcsin\left(\frac{r}{\sqrt{d^2+D^2}}\right)$ and $\arctan\left(\frac{d}{D}\right) - \arcsin\left(\frac{r}{\sqrt{d^2+D^2}}\right)$, respectively. Using the APSD given in Section 2, the *remaining* energy, which is a function of the shadowing position as shown in Fig. 3, can be calculated by:

$$E_r(d) = 1 - \int_{\theta_2(d)}^{\theta_1(d)} P(\theta) d\theta \tag{7}$$

where the total energy of the channel IR is normalized to 1. Here the distance D is fixed when the people moves along the straight line and thus is omitted in the expression for simpler denotation. Then the shadowing effect, (in terms of dB) is:

$$\chi(d) = 10\log_{10}[E_r(d)] \tag{8}$$

Further, the values of $\chi(d)$ can be obtained at a series of positions occupied by the people along the path.

The numerical results of the shadowing effect when the people is penetrating the LOS alone a straight path is shown in Section 6. Also, some realistic measurement of such shadowing effect can be found in [8]. Both of them show that the people shadowing introduces large attenuation on the received power and thus leads to significant degradation of system performance.

4 Markov model for UWB channel with people shadowing

Similar to the finite-state Markov chain (FSMC) channel model widely used in modeling the Rayleigh fading channel [9, 10], we can construct a Markov chain for describing the dynamics of the UWB shadowing channel at the packet level. The Markov channel model is characterized by two properties, the channel states and the state transition probabilities for discrete-time FSMC or transition rate for continuous-time FSMC. In this paper we will describe the continuous ones while it is easy to be mapped to the discrete ones.

4.1 The definition of channel states

The total received power decreases when the LOS is blocked, so does SNR since the SNR is proportional to the received power. The shadowing effect is large-scale fading which imposes a time-varying attenuation on the total received power, as obtained in Section 3. Following the approach in [10], we can partition the SNR into several non-overlap intervals and each interval is a state of the channel. According to the blocking model, each SNR interval actually corresponds to the spatial zone of the moving obstacle. In other words, once a person enters a particular zone, the channel is in corresponding state due to the shadowing, and the received SNR can be estimated accordingly. The average BER and PER can be further estimated from the average received SNR, which will be addressed later in the paper. The states of the Markov model can be obtained as follows.

First, let $\bar{\gamma_0}$ (dB) be the average received SNR when there is no shadowing. $\bar{\gamma_0}$ depends on the link budget of the UWB transmission system and will be evaluated in detail in Section 5. The resultant received SNR with shadowing effect depends on the position of the obstacle and can be obtained by:

$$\gamma(d) = \bar{\gamma_0} + \chi(d), \tag{9}$$

where $\chi(d)$ is defined in Eq. 8.

Second, divide the area near the LOS into N zones, $\Delta d_n, n = 0, 1, \cdots, N-1$, which correspond to N (an even number) states, S_n, as shown in Fig. 5. Note that the zones at the two ends actually belong to the same state S_0 because people is out of the shadowing region. The SNR interval of S_n is $[\Gamma_n, \Gamma_{n+1})$, where $\Gamma_n = \gamma(d_n)$ is the threshold to divide the SNR range and corresponds to the SNR when the people is at position d_n. N should be sufficiently large such that the range of SNR in each state should be small enough. Thus, we can use

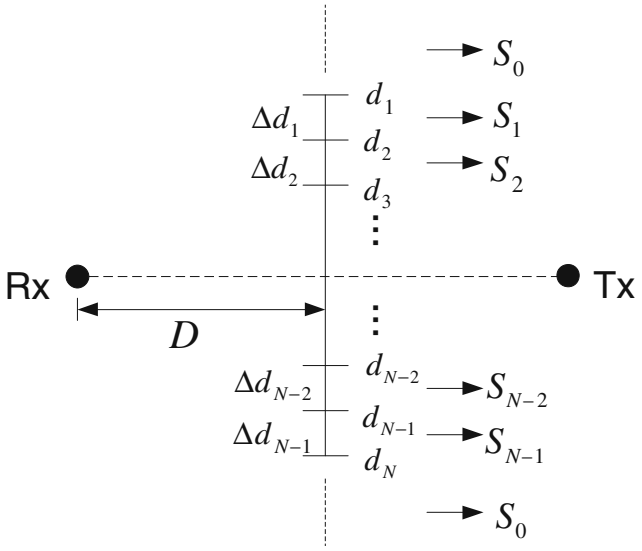

Figure 5 Two dimensional zones corresponding to channel state

the average SNR in that range, $\bar{\gamma_n}$, to represent the state S_n, and it can be obtained by $\bar{\gamma_n} = \bar{\gamma_0} - \bar{\chi_n}$ where $\bar{\chi_n}$ is the average shadowing effect of the state.

Because the APSD and the shadowing model are actually symmetric with respect to the LOS line as described earlier, the received power and SNR of zone n and zone $N-n$ are the same, i.e., state S_n is the same as state S_{N-n}, and the threshold $\Gamma_n = \Gamma_{N-n+1}$, $n = 0, 1, \cdots, N-1$.

The structure of the channel state is shown in Fig. 6. Each state corresponds to the attenuation factor due to shadowing, i.e., the ratio of the received power with shadowing to the power without shadowing. State $S_{N/2}$ is the worst one with the center of the obstacle on the LOS line. State S_0 is the best case that there is no shadowing effect, i.e., nobody near the LOS area. Therefore, the average attenuation factor of state 0 is $\bar{\chi_0} = 0$ dB.

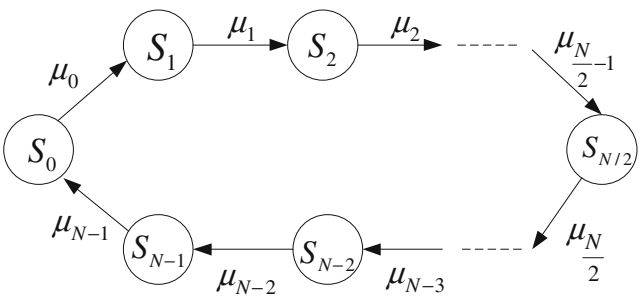

Figure 6 Packet-level model of time-varying UWB channel

4.2 State transition rate

The transition rate between the states is determined by the indoor mobility model of people and the geometric state zones. We investigate the process of a person walking along a path through the LOS in one direction with random speed: after the person enters zone 1 from zone 0, he/she will pass zone 2 to zone $N-1$, and finally re-enter zone 0.

First, since the channel state S_n corresponds to the zone $[d_n, \ d_{n+1})$, for $n = 0, 1, \cdots, N-1$, the travel length of each state is $\Delta d = d_{n+1} - d_n$. The instantaneous speed of the people is varying randomly and hence the duration of the people staying in one zone is a random variable. We assume that the time the person stays inside a zone is exponentially distributed. The average duration inside a zone is $\bar{t_n} = \frac{\Delta d_n}{\bar{v}}$, where $\bar{v}$ is the average speed of the person. Therefore, the transition rate from state n to state $(n+1) \mod (N)$ is

$$\mu_n = \frac{1}{\bar{t_n}} = \frac{\bar{v}}{\Delta d_n} \quad n = 1, 2, ..., N-1. \tag{10}$$

Again, because of the symmetry of the shadowing model, we have $\mu_n = \mu_{N-n}$.

Second, the transition from S_0 to S_1 actually means a person arrives and thus the LOS shadowing occurs. We assume that the arrival of a person is a Poisson process with the arrival rate of μ_0, which is determined by the density and mobility of the people inside the home or office. For example, in a more crowded area, we can set a higher value of μ_0, and vice versa. Also, from μ_0, we can obtain the average duration of the no-shadowing effect (the state S_0) by $\bar{t_0} = 1/\mu_0$.

Given the states and the state transition rate, a continuous-time Markov model of the UWB channel is obtained, as shown in Fig. 6.

4.3 Steady state probability

The steady state probability of the continuous-time FSMC can be obtained using the eigenvector method. Or, because the time duration of each state is exponentially distributed, the steady state probability of state n is proportional to $\bar{t_n}$:

$$\pi_n = \frac{\bar{t_n}}{\sum_{i=0}^{N-1} \bar{t_i}} \tag{11}$$

5 Performance of MB-OFDM network considering people shadowing

In the previous sections, the basic structure of the FSMC based packet-level model for UWB shadowing

channel has been established. Next, given that the channel is in a state, we study the PER and throughput of UWB systems. To illustrate the people shadowing effect to the network performance, we consider Multi-Band OFDM (MB-OFDM) [11] system in the rest of the paper and our approach is ready to be extended for other UWB systems.

5.1 MB-OFDM system

MB-OFDM (recently has been standardized by ECMA [12]) is a promising technology due to the maturity of high rate OFDM technology and its flexibility to spectrum regulations.

Multiband OFDM is a conventional OFDM system combined with bit-interleaved coded modulation for error prevention and frequency hopping to improve diversity. The multiband approach divides the available UWB spectrum into several subbands that occupy 528 MHz each and contains 128 subcarriers. The interleaved and convolutional coded bits are mapped to QPSK symbols and groups of 100 data symbols form OFDM symbols by 128 point IFFT. Time and frequency domain spreading is used to reduce the effective code rate by a factor of two each and provide an additional spreading gain for low data rate modes.

One OFDM symbol has a duration of $T_{SYM} = T_{FFT} + T_{CP} + T_{GI} = 312.5$ ns where $T_{FFT} = 242.4$ ns is the FFT integration time, $T_{CP} = 60.61$ ns is the length of the cyclic prefix and $T_{GI} = 9.47$ ns is the guard interval.

On a larger scale, transmission is organized in packets of varying payload length. The MB-OFDM proposal has specified the structure of the physical layer convergence protocol (PLCP) frame, as shown in Fig. 7a. The transmission time for a PHY packet is (in the unit of μs):

$$T_P = T_{Pre} + T_H + N_{SYM} \times T_{SYM}, \tag{12}$$

where T_{Pre} is the transmission time for the PLCP preamble, which is 9.375 μs (30 OFDM symbols) in normal mode or 5.625 μs (18 symbols) in streaming mode, and $T_H = 3.75$ μs is the transmission time for the PLCP header which is padded out to 12 symbols and is always sent at an information data rate of 55 Mbps. The number of OFDM symbols in the PHY payload, N_{SYM}, is determined by the length of link-layer frames, the spreading factors and the coding rate [11]. In addition, the interframe spacing should also be considered. The Tx/Rx turnaround time is defined as $T_{SIFS} = 10$ μs. The time between uninterrupted successive transmissions by the same device shall be $T_{MIFS} = 1.875$ μs.

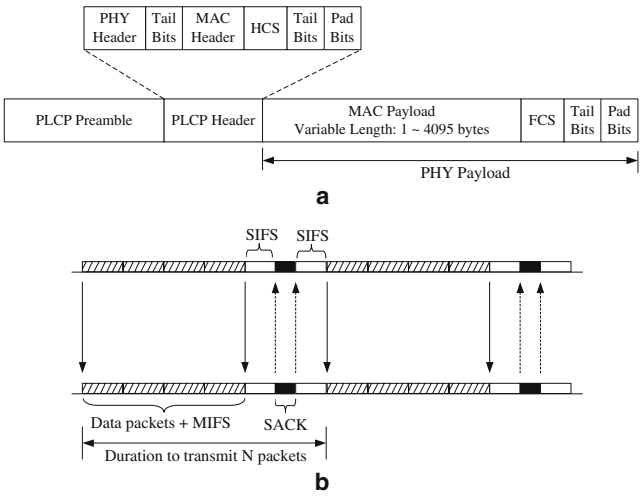

Figure 7 Packet transmission a peer-to-peer MB-OFDM link. **a** PLCP frame format. **b** SR-ARQ scheme with window size of $W = 4$ packets

The frame structure and timing are used throughout the paper to analyze the link performance of the MB-OFDM system.

5.2 Estimation of PER of MB-OFDM system

We first evaluate the PER of MB-OFDM systems, since the following formulation of link performance (throughput and delay) is based on the PER, which in turn is determined by the received SNR $\gamma = E_b/N_0$.

Due to the complexity of realistic UWB channels and practical transmission systems, it is very difficult to obtain the close-form of accurate BER or PER. In the literature, some forms of BER are derived by assuming simplified channels like AWGN or stochastic time delayed line models and simplified transceiver systems. On the other hand, the complete performance simulations are given in the MB-OFDM PHY system proposal [11]. The performance results not only are based on realistic UWB channel realizations specified by the 3a channel model, but also use the practical implemented system and incorporate losses due to front-end filtering, clipping at the DAC and ADC degradation, packet acquisition, channel estimation, carrier tracking, etc. Therefore, in order to reflect the performance of the practical implemented MB-OFDM system over a realistic UWB channel, we use the system simulation results provided by the proposal [11] and adopt the numerical approximation method to obtain the PER [13]. Consequently, given the received SNR, the PER can be obtained.

The performance results given in [11] are in terms of PER versus distance. Since the path loss model defined

in 3a model [4] (with decay exponent of two) is used in the simulations, we can determine the received SNR at distance d according to the link budget, as:

$$\gamma = P_T - L(d) - N - N_F - I + X_{dB}, \tag{13}$$

where the system noise figure $N_F = 6.6$ dB, implement loss $I = 2.5$ dB, and $N = -174 + 10\log_{10}(R_b)$ is the thermal noise per bit where R_b is the information data rate. The transmission power is $P_T = -10.3$dBm. $L(d)$ is the path loss defined as $L(d) = 20\log_{10}\frac{4\pi f_c' d}{c}$, where f_c' is the geometric center frequency of the signal. The term X_{dB} is the total channel attenuation which is defined in the 3a channel model as $X_{dB} = 20\log_{10}(X) \sim N(0, \sigma_X)$.

The system performance for the 90^{th}%ile channel realization is usually of interest and used in the simulation in [11], which corresponds to the performance of the 90th best one of the 100 random channel realizations. Since the channel condition and thus the link success probability are dominated by the large-scale fading and not by the signal acquisition (the multipath profile and small-scale fading) in MB-OFDM [11], the 90^{th}%ile channel realization can be found by setting $F(X_{dB}) = Q(X_{dB}/\sigma_X) = 0.9$, where $Q(x) = \frac{1}{\sqrt{2\pi}}\int_x^\infty \exp\left(-\frac{t^2}{2}\right) dt$ and $\sigma_X = 3$ dB [4]. We can get $X_{dB} = -3.84$ dB. We will use Eq. 13 to obtain the SNR of the 90^{th}%ile channel realization in this paper.

The PER performance of 110 Mbps MB-OFDM in 3a CM1 from [11] is plotted on a semi-log graph in Fig. 8. The observation suggests that we can split the PER curve into three segments. Using the same approach in [13], each segment is fitted with an exponential curve (straight lines on the semi-log graph). Thus, the PER, ϵ, can be expressed as (with payload length of 1000 bytes):

$$\epsilon(\gamma) = 10^{a_i\gamma + b_i} \tag{14}$$

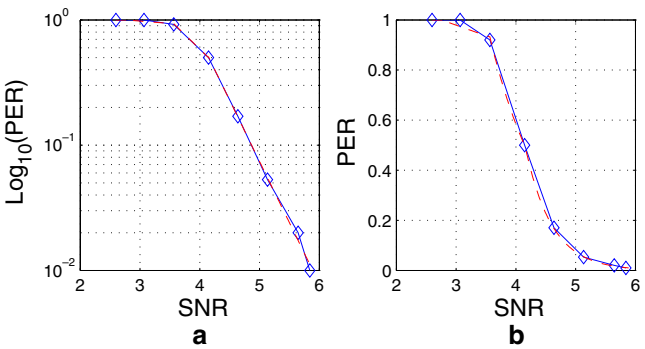

Figure 8 PER of MB-OFDM system in 3a CM1 channel environment (**a**, **b**) (– ◇ –: simulation results [11]; – –: linear regression approximation)

Table 1 Coefficients and splitting points of curve fitting

Segments SNR	Range (dB)	a_i	b_i
1	0 – 3.56	−0.0378	0.1041
2	3.56 – 4.15	−0.4657	1.6294
3	4.15 – 5.84	−0.9769	3.7547

The coefficients, a_i and b_i, for each segment are separately obtained using linear regression on SNR γ and logarithm of ϵ. The values of coefficients and the splitting points, γ_i, are listed in Table 1. As shown in Fig. 8, our best fit curve with three segments is close enough to the actual PER values.

5.3 SR-ARQ protocol and link layer performance evaluation

We consider the performance of a peer-to-peer MB-OFDM link, and the truncated Selective Repeat Automatic Repeat reQuest (SR-ARQ) is used for error recovery in the link layer.

We assume that the MAC frame length is 0 ∼ 1500 bytes (the maximal payload length of Ethernet frame). Hence a link-layer frame is encapsulated into one PLCP packet and transmitted. At the receiver, the MAC frame is extracted from the PLCP packet, submitted to link-layer and checked with errors. Note that in the physical-layer, only the combined PLCP and MAC headers are checked with CRC-16 header check sequence.

SR-ARQ is selected in order to obtain the highest throughput when the channel is erroneous and with high data rate. After a full sender's window of packets have been transmitted, the receiver sends back the selective-ACK (SACK) and instructs the transmitter to resend only the packets that contained errors. One packet is re-transmitted at most K times. Figure 7b shows the SR-ARQ protocol used in the link layer. The packet sending rate, R_t, can be obtained as:

$$R_t = \frac{W}{WT_P + (W-1)T_{MIFS} + 2T_{SIFS} + T_{ACK}} \tag{15}$$

where W is the window size in packets, and the transmission time of data packet (T_P) and ACK packet (T_{ACK}) are determined by Eq. 12.

Given the length of the MAC payload, i.e. L bits, and the PER ϵ, the throughput of the SR-ARQ scheme is:

$$H = (1-\epsilon)R_t L \tag{16}$$

where $(1-\epsilon)R_t$ gives the number of correctly received packets per second. This expression of the link throughput is used to evaluate the MB-OFDM system with people shadowing effect in the following numerical results.

To investigate the delay of the MB-OFDM link, the transmitter with finite buffer size is analyzed using a queueing process. Given truncated SR-ARQ with retry limit of K and the PER of ϵ, the probability of a packet being retransmitted k times is:

$$p_t(k) = \begin{cases} \epsilon^k(1-\epsilon), & k = 0, 1, \cdots, K-1 \\ \epsilon^K & k = K \end{cases} \tag{17}$$

The average number of transmission and retransmissions of one packet can be obtained by:

$$N_t = \sum_{k=0}^{K} k p_t(k) = \frac{1-\epsilon^{K+1}}{1-\epsilon} \tag{18}$$

Then, the average service time of one packet is $T_s = N_t/R_t$ where R_t is given by Eq. 15.

Because the distribution of the packet service time depends on the probability of number of retransmissions in Eq. 17, the service time is not exponentially distributed, and results in a G/G/1 queue. Since we focus on the system performance when the channel is degraded and the service rate is less than the arrival rate, we assume that the buffer is full in this period. Based on the average service time for one packet, the total delay, including the queueing delay and service time, is approximated by (the buffer size is B packets):

$$T_D = BT_s + T_s \approx (B+1)\frac{1-\epsilon^{K+1}}{(1-\epsilon)R_t}. \tag{19}$$

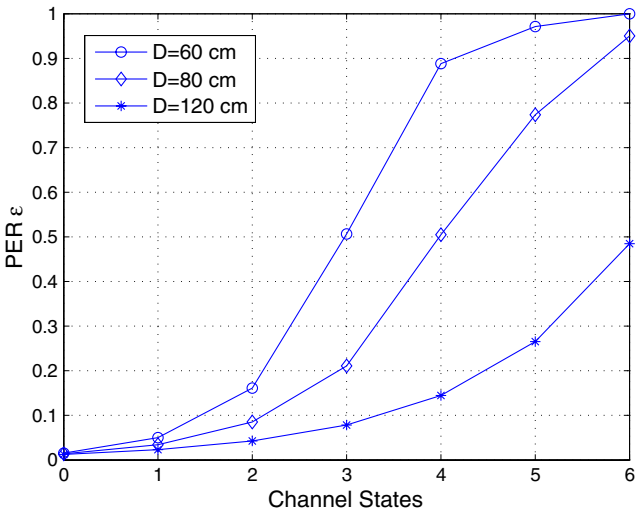

Figure 10 PER with people shadowing effect for different distances between the people and Rx

In summary, multiple channel states are defined based on different shadowing effect. First, for the state S_n, we can obtain the average shadowing effect for this state, $\bar{\chi_n}$, based on the UWB channel APSD and the shadowing model described in Section 3. Then, from Eq. 14, the average PER $\bar{\epsilon_n}$ can be acquired. Third, by plugging $\bar{\epsilon_n}$ into Eq. 16 and 19, the UWB link performance of throughput and delay for state S_n can be obtained, respectively. Each channel state is associated with the link throughput/delay. Finally, the transition between the channels states due to the people movement causes the variation of the UWB channel and thus the link performance.

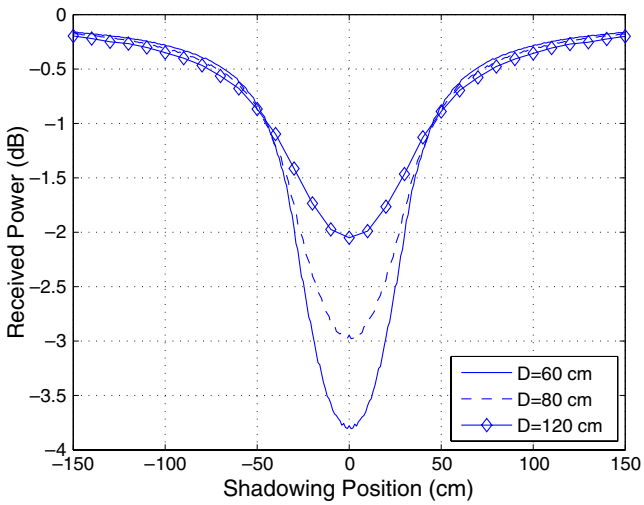

Figure 9 Power attenuation by the shadowing of moving people for different distances between the people and Rx

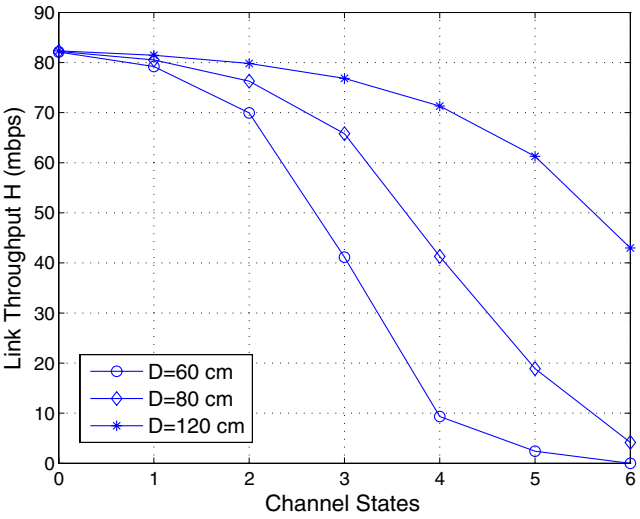

Figure 11 Throughput with people shadowing effect for different distances between the people and Rx

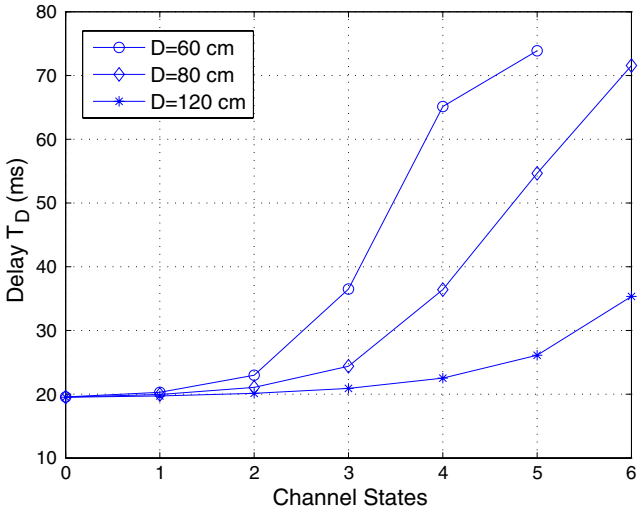

Figure 12 Delay with people shadowing effect for different distances between the people and Rx

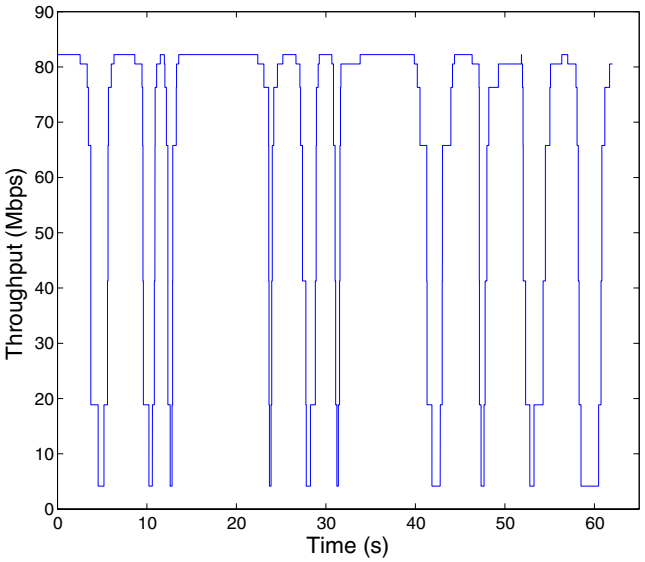

Figure 13 Throughput fluctuation of peer-to-peer MB-OFDM link due to shadowing effect

6 Numerical results

To demonstrate the people shadowing effect and the proposed Markov channel model, numerical results are given in this section. We consider the scenario that stationary Tx and Rx are deployed, with the distance of 10m in between and the data rate of the MB-OFDM system is 110 Mbps (according to the data rate versus ranges requirement of UWB systems). People randomly arrive and penetrate the LOS along a straight path, as shown in Fig. 3. The link-layer uses SR-ARQ with window size $W = 4$ packets and the maximum number of retransmissions $K = 3$. The Markov model of $N = 12$ states is used here.

6.1 Shadowing effect

Calculations are taken at a series of positions along the path perpendicular to the LOS. The sampling starts at $d = 1.5$m and ends at 1.5m on the other end of the path. The averaged shadowing effect according to Eq. 8 is shown in Fig. 9. In order to show the different shadowing situation, the results for people moving along a path with different distance D from receiver (Rx) are calculated. The results obtained by the analytical model reasonably match the measurement given in [8].

6.2 Channel states

From the estimation of link budget in Eq. 13, the received SNR without shadowing can be obtained as $\bar{\gamma_0} = 6.1185$dB. Based on the shadowing effect obtained above, shadowed SNR can be got by Eq. 9. Then we divide the SNR range into $\frac{N}{2} + 1 = 7$ intervals equally, and each interval corresponds to a channel state. We use the average SNR to represent the channel state and thus obtain the average PER, throughput and delay. State 0 corresponds to the situation that there is no people near the LOS and thus no shadowing effect. State 6 corresponds to the worst situation that the center of the people is on the LOS and therefore the shadowing effect is most severe. The results are shown in Figs. 10, 11 and 12, respectively.

The numerical results have shown that the shadowing of a person's body makes significant effect on

Table 2 Parameters for the Markov model (State S_{N-n} and state S_n are identical, $n = 1, 2, \cdots, N-1$)

n	0	1	2	3	4	5	6
$N-n$		11	10	9	8	7	
$\overline{\chi_n}$ (dB)	0	−0.7760	−1.1798	−1.5831	−1.9824	−2.3803	−2.7781
SNR $\overline{\gamma_n}$ (dB)	6.1185	5.3426	4.9388	4.5354	4.1362	3.7382	3.3405
PER $\overline{\varepsilon_n}$	0.006	0.0343	0.0851	0.2109	0.5049	0.7736	0.9502
Δd_n (cm)	–	19	10	7	5	8	32
μ_n(/s)	0.5	2.153	4	5.7143	8	5	1.25
π_n	0.381	0.0905	0.0476	0.0333	0.0238	0.0381	0.1524

the PER which increases obviously when the person blocks the LOS gradually, and thus degrades the link performance severely.

6.3 Markov channel model

As an example, we consider that people randomly penetrate the LOS (i.e. random arrive) with random speed along a straight path with distance to Rx of $D = 0.8$m. People has Poisson arrival with arrival rate of $\mu_0 = 0.5$ per second and the average moving speed is $\bar{v} = 0.4$ m/s. According to Section 4, the Markov channel model can be established. The parameters for the model are listed in Table 2.

The steady state probabilities of the continuous-time FSMC are obtained using Eq. 11. As we can see, the steady state probabilities depend on the people arrival rate μ_0. When μ_0 is small, the LOS shadowing happens occasionally and therefore the probability of the good channel state is high; when μ_0 is large, the LOS shadowing happens frequently, the probabilities of the shadowing states raised.

Figure 13 illustrates the fluctuation of the throughput of the peer-to-peer MB-OFDM system. People randomly pass through the LOS and the Markov model is used to generate the random link throughput. The variation of the throughput from 80 Mbps to less than 20 Mbps or worse can be observed frequently.

7 Conclusions

In this paper, we have investigated UWB indoor channels with people shadowing processes, and proposed a packet-level model for the time-variation of the UWB channel using the following steps. First, the shadowing processes have been quantified using the angular power density spectrum and the human blocking model, which are recommended by the IEEE802.15 WPAN group. Numerical results of the shadowing effect have been given. The average received signal power matches the practical measurement results. Second, the received SNR can be partitioned into multiple intervals and each interval corresponds to a channel state. The two dimensional space around the Tx and Rx is divided into different zones corresponding to different states. Third, given the mobility model, the state transition rate can be obtained and thus the Markov channel model is constructed. The model can be applied for both DS-UWB and MB-OFDM UWB networks. Because of the low computation requirements, the channel model is simple and feasible to be incorporated to existing network simulators like NS-2 or GloMoSim. Network researchers can use the model to investigate the performance of UWB networks and upper-layer protocols analytically and via simulation.

Although we use a simple mobility model as an example in the paper, the channel model is ready to be extended considering more complicated mobility models. This paper focuses on the shadowing effect, so channel states corresponds to geometric zones of people's positions. In the future, we plan to build a simple packet-level channel model considering both the shadowing effect and the channel fading statistics. How to extend the packet-level model of UWB channel considering the mobility of transmitter or receiver is under investigation.

References

1. Saleh A, Valenzuela R (1987) A statistical model for indoor multipath propagation. IEEE J Sel Areas Commun 5(2): 128–137, February
2. Spencer Q, Jeffs B, Jensen M, Swindlehurst A (2000) Modeling the statistical time and angle of arrival characteristics of an indoor multipath channel. IEEE J Sel Areas Commun 18:347–360, March
3. Cramer RJ, Scholtz RA, Win MZ (2002) Evaluation of an ultra-wide-band propagation channel. IEEE Trans Antennas Propag 50(5):561–570, May
4. IEEE802.15.SG.3a (2005) Channel modeling sub-committee report final. IEEE 802.15-02/490rl-SG3a, February
5. Zhuang W, Shen X, Bi Q (2003) Ultra-wideband wireless communications. Invited tutorial paper. Wirel Commun Mob Comput 3(6):663–685 (special issue on ultra-broadband wireless communications for the future)
6. Molisch A et al (2004) IEEE 802.15.4a channel model – final report. IEEE TG802.15.4a, 15-04-0662-08-004a, November
7. Molisch A (2002) Time variance for UWB wireless channels. IEEE P802.15-02/461-SG3a and IEEE P802.15-02/462-SG3a
8. Schell SV (2002) Analysis of time variance of a UWB propagation channel. IEEE P802.15-02/452-SG3a and IEEE P802.15-02/453-SG3a
9. Wang HS, Moayeri N (1995) Finite-state Markov channel: a useful model for radio communication channels. IEEE Trans Veh Technol 44(1):163–171, February
10. Zhang Q, Kassam SA (1999) Finite-state Markov model for Rayleigh fading channels. IEEE Trans Commun 47(11): 1688–1692, November
11. Batra A et al (2004) Multi-band OFDM physical layer proposal for IEEE 802.15 task group 3a. IEEE 802.15-04/0493rl, September
12. ECMA (2005) Standard ECMA-386: high rate ultra wideband PHY and MAC standard. Ecma standard. The WiMedia specification. ECMA, The Hague
13. Nguyen GT, Noble B, Katz RH, Satyanarayanan M (1996) A trace-based approach for modeling wireless channel behavior. In: Proc. 1996 winter simulation conference, pp 597–604, Coronado, 8–11 December 1996

Ruonan Zhang received the B.S. and M.S. degrees in electrical engineering from Xi'an Jiaotong University, Shaanxi Province, China, in 2000 and 2003, respectively. He was with Motorola Inc. and later with Freescale Semiconductor Inc. in Tianjin, China, from 2003 to 2006, working on IC architecture and application design. He is now working toward the Ph.D. degree at the Department of Electrical and Computer Engineering, University of Victoria, British Columbia, Canada. His current research interests include cross-layer design and optimization for wireless networks and wireless personal area network (WPAN).

Lin Cai received the M.A.Sc. and Ph.D. degrees (with Outstanding Achievement in Graduate Studies Award) in electrical and computer engineering from the University of Waterloo, Waterloo, Canada, in 2002 and 2005, respectively. Since July 2005, she has been an Assistant Professor in the Department of Electrical and Computer Engineering at the University of Victoria, British Columbia, Canada. Her research interests span several areas in wireless communications and networking, with a focus on network protocol and architecture design supporting emerging multimedia traffic over wireless, mobile, ad hoc, and sensor networks. She serves as the Associate Editor for IEEE Transactions on Vehicular Technology (2007-), EURASIP Journal on Wireless Communications and Networking (2006-), and International Journal of Sensor Networks (2006-).